Technical Paper 3649

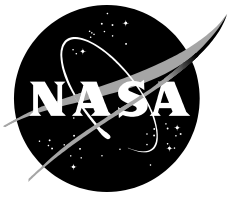

Measurement and Validation of Bidirectional Reflectance of Space Shuttle and Space Station Materials for Computerized Lighting Models

Lauren E. Fletcher, Ann M. Aldridge, Charles Wheelwright, and James Maida

March 1997

Technical Paper 3649

Measurement and Validation of Bidirectional Reflectance of Space Shuttle and Space Station Materials for Computerized Lighting Models

Lauren E. Fletcher, Ann M. Aldridge, and Charles Wheelwright
Lockheed Martin Engineering and Science Services
Houston, Texas

James C. Maida
Lyndon B. Johnson Space Center
Houston, Texas

March 1997

Acknowledgments

This research was supported by funding from the Johnson Space Center Center Director's Discretionary Fund.

Many people have provided invaluable contributions to this project. The authors would like to especially thank the following people: Abhilash Pandya (Graphics Research and Analysis Facility, or GRAF) for assistance in developing GRAF's lighting capabilities, spending many hours exploring different computer models to determine which programs would be beneficial to GRAF; Lorraine Hancock (GRAF) for help with early attempts at "band-aid" repairs on the goniorefectometer; Jennifer Toole (Lighting Environment Test Facility) for an initial compilation of lamp data for the Space Shuttle and Space Station Freedom; Jack Aldridge for spending many hours reading and making suggested changes to this report; and especially Greg Ward at Lawrence Berkeley Laboratory for his help in using Radiance with the GRAF software system.

This publication is available from the NASA Center for AeroSpace Information,
800 Elkridge Landing Road, Linthicum Heights, MD 21090-2934, (301) 621-0390

Contents

Contents

(continued)

Contents

(concluded)

Page

Figures

Acronyms

BCP	Beam candle power
BR	bidirectional reflectance
BRDF	bidirectional reflectance distribution function
CETA	crew equipment translation assembly
CTVC	color tv camera
EMU	extravehicular mobility unit
EVA	extravehicular activity
GRAF	Graphics Research and Analysis Facility
HAB	habitation module
HST	Hubble Space Telescope
HWHM	half-width half-maximum
ISS	International Space Station
LETF	Lighting Environment Test Facility
MLA	monochromatic lens assembly
ODS	Orbiter docking system
OHDFL	over head docking floodlight
RMA	remote manipulator assembly
SSMTF	Space Station Mockup and Training Facility
STS	Space Transportation System

Abstract

Task illumination has a major impact on human performance: What a person is able to perceive in his environment significantly affects his ability to perform tasks, especially in the harsh environment of space. For many years, training for lighting conditions in space has depended on physical models and simulations to emulate the effect of lighting on space operations. But such tests are expensive and time-consuming to set up. To evaluate lighting conditions not easily simulated on Earth, personnel at NASA's Graphics Research and Analysis Facility (GRAF) at the Johnson Space Center (JSC) have been developing the capability to provide computerized simulations of various illumination conditions using the ray tracing program, Radiance, developed by Greg Ward at Lawrence Berkeley Laboratory. Because these computer simulations are only as accurate as the data used, accurate information about the reflectance properties of materials and light distributions is needed.

JSC's Lighting Environment Test Facility (LETF) personnel gathered material reflectance properties for a large number of paints, metals, and cloths used in the Space Shuttle and Space Station programs. These data were processed into reflectance parameters needed for the computer simulations. Lamp distribution data were gathered for most of the light sources used in the Space Shuttle and Space Station programs. LETF personnel also validated the ability to accurately simulate lighting levels by comparing predictions with measurements for several ground-based tests.

The result of this study is a database of material reflectance properties for a wide variety of materials, and lighting information for most of the standard light sources used in the Space Shuttle and Space Station programs. The combination of the Radiance program and GRAF's graphics capability form a validated computerized lighting simulation capability for NASA.

1.0 Introduction

Awareness of surroundings critically impacts an astronaut's ability to carry out assigned tasks. Perception of surroundings in space is more difficult than on Earth because the lack of atmospheric scattering of light causes very high contrast and sharp-edged shadows to occur. Problems with glare and rapid changes between bright sun light and orbit night during the time of a task also occur. Television cameras, used in numerous on-orbit tasks, pose special problems due to their lower dynamic range compared to the human eye. Evaluation of lighting conditions for performance of on-orbit tasks and training with realistic lighting are important to successful Space Shuttle missions and the assembly of the Space Station.

Since the Gemini program, NASA's Johnson Space Center (JSC) has used ground-based mockup testing and scale models to evaluate on-orbit illumination and to provide training for astronauts. Some of these procedures are very expensive to carry out and only partially simulate the actual conditions. With the impending Space Station assembly sequences, a more efficient means of conducting lighting analyses was needed. The Graphics Research and Analysis Facility (GRAF) has combined its modeling and graphical interfaces with a lighting model computer program, Radiance, developed at Lawrence Berkeley Laboratory to perform accurate, rapid ray tracing calculations for reflected and diffuse light from multiple surfaces. This new capability permits the computational prediction of light levels on surfaces in complex configurations for visibility or viewing analysis. The sun, diffuse earth shine, and/or a collection of vehicle-based lights may be used as illumination sources.

Successful use of the GRAF lighting modeling [1] depends on having material properties that describe the reflection of light from various spacecraft structures. Such information includes overall reflectivity of the surface, the distribution of the reflected light in each direction from the material surface, and the distribution of the incident light being reflected. This report discusses measurements made in the Lighting Environment Test Facility (LETF) to provide the data for a variety of lamps and materials.

Computed lighting levels (luminance from surfaces and illumination on surfaces) were validated by comparing computed values to measurements made during ground-based lighting tests. Two tests were coordinated with training simulations for the Space Transportation System 71 (STS-71) and STS-74 Shuttle-*Mir* docking maneuvers. One of these tests used a solar simulator to model sun lighting conditions on the docking target. The other test modeled artificial lighting from the Orbiter docking system (ODS) to simulate night illumination on the docking target. A third test measured interior lighting levels in a Space Station mockup of the habitation (HAB) module. The GRAF modeling could reliably predict lighting levels for these interior and exterior environments.

Section 2 discusses the reflectivity parameterization in the Radiance program, the methods of making these measurements, and the processing of the data measurements into the Radiance reflectivity parameters. Section 3 discusses the light distribution parameters needed for the Radiance program, and methods for obtaining these parameters. Section 4 presents the results from three validation tests. Appendix A contains lamp distributions.

2.0 Material Reflectance Data

The section below discusses how light is reflected from a material surface and the parameters Radiance uses to model this reflection. Also, the method used in this project to measure the material reflectance distribution is discussed. Finally, we discuss how these measurements were processed into the parameters needed for the Radiance computer program.

2.1 Theory

Radiance[1] is a public domain software tool for analyzing lighting levels from multiple light sources. It is a backwards ray-tracing program in which rays from the point-of-entry of an eye or camera are traced until they encounter some object. If this object is a light, then the luminance from the light into the eye is directly calculated. Otherwise, the object, at the point at which the eye ray strikes it, will generate rays from this surface to "look" for a light source. If a light source is found, its illumination on the object is determined, and the reflective properties of the object surfaces are used to determine how much of this light is reflected from the object into the eye. If the new rays strike another object instead of encountering a light, the backward ray-tracing process will continue until a light source is found or until a prescribed number of reflections is exceeded. Specular reflectance, which occurs only at an angle equal to the angle of incident, is easy to trace. This method of tracing rays backwards can be computationally expensive for surfaces with diffuse scattering because light is reflected in all directions. Radiance has developed random sampling techniques to speed up this process of tracing diffuse reflections [2].

To describe the reflectivity of a material accurately, it is necessary to model the ratio of the reflected light intensity to the incident light intensity at any angle in a hemisphere above the plane of the reflecting surface[2]. This ratio of the reflected light, collected by a small detector, to the collimated incident light is the bidirectional reflectance (BR). The value of BR depends on the spherical angles of the reflected light to the surface of the material and reflectance property of the material. It also is proportional to the size of the solid angle of the detector.

---

[1] Radiance was developed by the Lighting Group at Lawrence Berkeley Laboratory with Greg Ward, Program Manager and principal author. Funding for this project was provided by the U.S. Department of Energy and The Laboratoire d'Energie Solaire et de Physique du Batiment at the Ecole Polytechnique Federale de Lausanne, Switzerland.

[2] Complex graphical objects consist of "polygons" that are planar approximations to the actual surfaces at a particular location. These polygons are generated at a size to produce a specified accuracy of approximation to the physical surface.

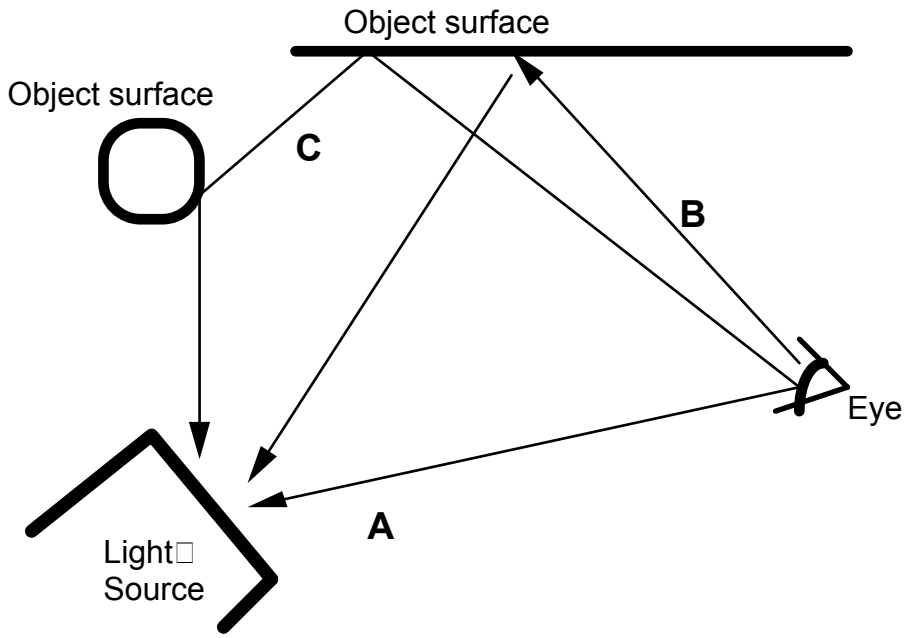

Figure 2.1: The backward tracing of rays directly to the light [A] and indirectly from the material surface by one [B] or more [C] reflections.

If a plot of the BR for a perfectly diffuse material is made, the curve shows a cosine intensity distribution with respect to the normal to the surface. We can derive the bidirectional reflectance distribution function (BRDF) from the BR measurement. This BRDF, defined as the ratio of the reflected luminance to its incident illumination, is obtained by dividing the BR value at each angle by the cosine of the vertical angle and dividing by the small solid angle of the detector. Note that a plot of BRDF for a perfectly diffuse material will be a constant at all angles. A plot of the BRDF for materials with both diffuse and specular components should have a constant component in the diffuse region while the BRDF increases to a peak in the specular region. The peak occurs at the angle of incident equal to the angle of reflection[3].

While theoretical models have been developed to model the reflectance characteristics of a material in terms of the structure of the material surface [3], they are not often used because of their complexity. Radiance provides a simple formula to describe the measured reflectance data. This model describes the total reflectance in terms of a constant (diffuse component) and a peaked distribution centered at the specular angle (specular component) which is described with a peak amplitude and a width. All three parameters can be estimated from measurements of the BRDF. The Radiance program [4] computes the interaction of light with a surface using the

[3] Incident light that is absorbed by the surface is reradiated as heat and does not contribute to the detected intensity. The diffuse reflection is assumed to arise from processes such as reflections from small particles or reflections in small crevices that randomize the incident light directions. The specular peak possesses a distribution because the normal, if the surface is viewed at a very fine resolution, points in a slightly different direction from the large-scale normal to the surface. Because the specular reflection actually occurs with respect to the microscopic surface, the specular peak appears broadened.

BRDF. This is a function of 2 incident angles and 2 reflected angles. The reflected luminance can be calculated using the following equation:

$$L_r(\theta_r,\phi_r) = \int_{0}^{2\pi}\int_{0}^{\pi/2} L_i(\theta_i,\phi_i) \bullet r_{bd}(\theta_i,\phi_i : \theta_r,\phi_r) \bullet \cos\theta_i \bullet \sin\theta_i d\theta_i d\phi_i \qquad (1)$$

where:

θ_i, θ_r is the vertical angle between the surface normal and the incident ray, reflected ray.

φ_i, φ_r is the azimuthal angle measured about the surface normal for the incident ray, reflected ray.

$L_i(\theta_i,\phi_i)$ is the incident luminance in units of energy/sec/area/solid angle.

r_{bd} is the BRDF function in units of (solid angle) $^{-1}$.

Radiance's empirical representation of the BRDF function contains a diffuse component, r_d, which as a constant term; a specular component which has a Gaussian distribution described in terms of an amplitude r_s; an angle δ between the normal vector and the half vector, h; and α which is the standard deviation of the surface slope (Figure 2.2). The surface slope term α is related to the roughness of the surface and is measured by the Gaussian width of the specular component.

$$r_{bd}(\theta_i,\phi_i : \theta_r,\phi_r) = \frac{r_d}{\pi} + r_s \bullet \frac{1}{\sqrt{\cos\theta_i \cos\theta_r}} \bullet \frac{\exp\left[-\tan^2(\delta)/\alpha^2\right]}{4\pi\alpha^2} \qquad (2)$$

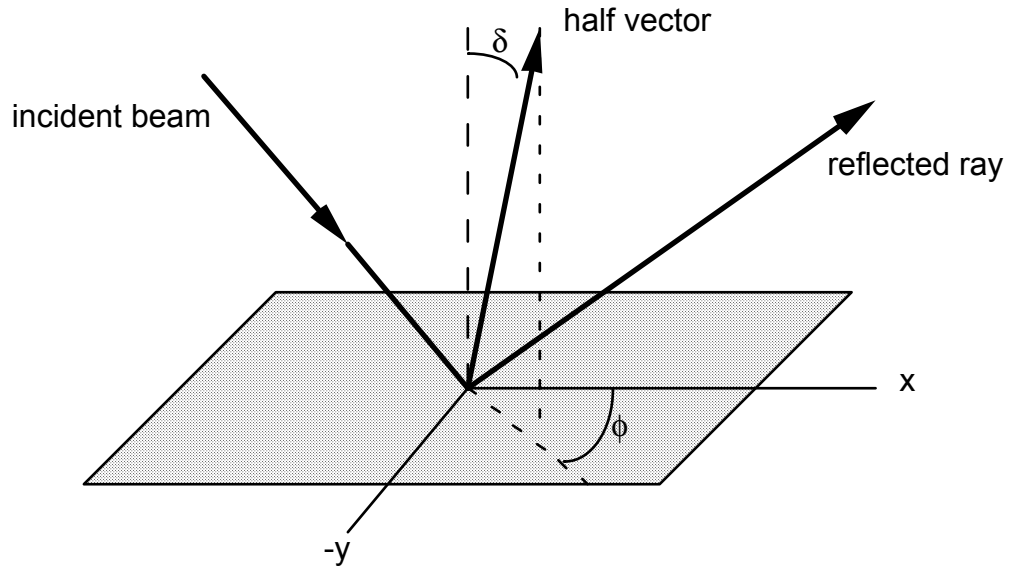

Figure 2.2: Geometry used in reflectance equation showing the direction of the incident and reflected light in terms of δ, the polar angle between the half vector h and the surface normal. The half vector is a unit vector corresponding to the microscopic normal at the point of reflection.

Some materials do not have an isotropic Gaussian reflectance but reflect light differently in different azimuthal directions. Materials with ribbed or brushed surfaces often show this characteristic. The Radiance model has extended its isotropic Gaussian model to a simple anisotropic[4] Gaussian model with two perpendicular slope distributions, α_x and α_y. This allows reflectance distributions which are elliptical instead of spherical. The specular exponential term is expanded

$$\text{from} \quad \left(-\tan^2(\delta/\alpha^2)\right) \qquad \text{to} \quad -\tan^2(\delta)\left(\cos^2\phi/\alpha_x^2 + \sin^2\phi/\alpha_y^2\right) \tag{3}$$

A more intuitive description of the peak width is the number of degrees from the peak angle of reflectance that the material will spread the light to half of the peak amplitude. This width in degrees is referred to as the half-width half-maximum (HWHM) of the Gaussian distribution for all measurements in this report.

2.2 Data Collection

A device for measuring the BR is a gonioreflectometer, which collects reflected values from a material sample over the angles in a hemisphere. The gonioreflectometer used to gather data for the calculation of BRDF for this project was a converging beam system constructed in accordance with ANSI/ASTME 167-77, developed and built by Lighting Sciences, Inc. [5]. It uses a high quality collimated light source and photodetector in a closed housing. The light source can be manually set to any stationary vertical angular setting from 90 to 0 degrees (Figure 2.3). The photodetector is attached to a computer-controlled, movable arm which can move to any vertical setting θ_r between 0 and ± 90 degrees. The arm is attached to a rotating turntable that is computer-controlled to move to any horizontal angle φ_r setting. This combination of the vertical and horizontal angular settings allows a full hemispherical coverage of reflected light.

A sample is set on a post at the center of rotation of the photodetector and light source. The height of the sample material on this post is critical in order to preserve the gonioreflectometer geometry. Because of this, the maximum thickness of the sample cannot exceed 0.25 inches (0.636 cm). If the sample is not thick enough, metal shims are used to boost the sample to the correct height. If the sample is too thick and cannot be cut down any further, the center post can be removed, but then the sample must be boosted to a total distance of 16.14 inches (41 cm) from the bottom plate of the housing.

[4] For a rough surface, the angle of the microscopic surface should be randomly distributed with a standard deviation measuring the degree of roughness. When the surface is treated in a particular direction (such as brushed or rolled), this approximation may not be an adequate description of the surface.

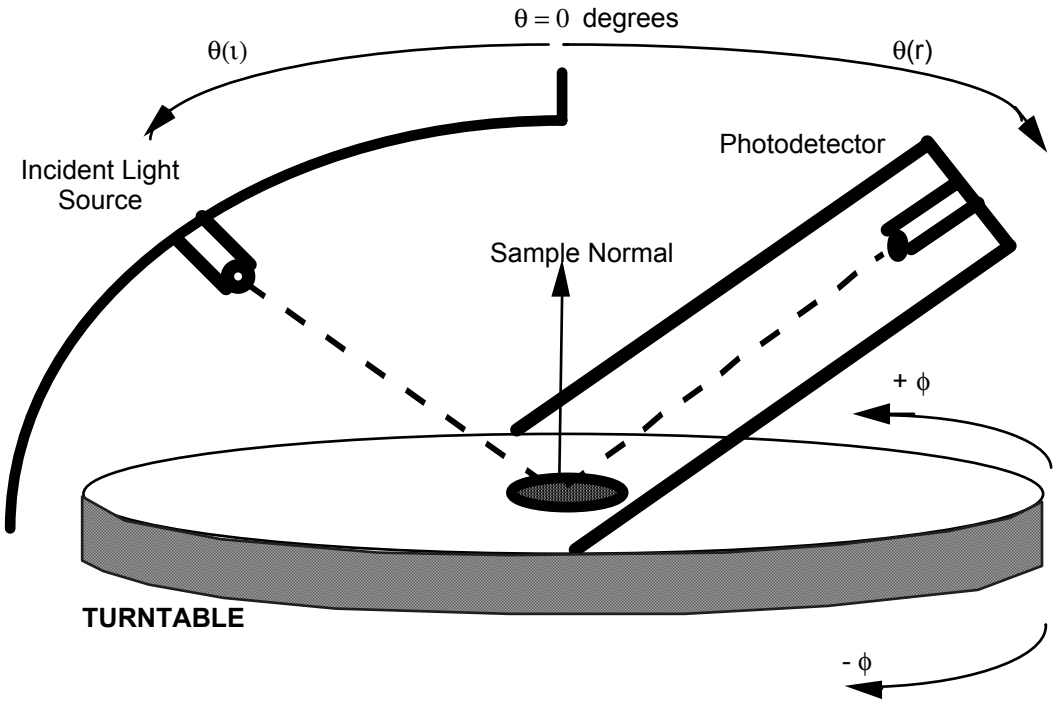

Figure 2.3: Gonioreflectometer basic components.

A series of calibration procedures were followed before data collection to ensure the validity of each sample run. The gonioreflectometer was warmed up for at least 30 minutes to allow both the light source and the photodetector to become thermally stabilized. Following the warm-up period, the gonioreflectometer was calibrated with a standard plaque of white porcelain enamel with a known BRDF.

The computer interface allowed data collection over a variety of angles at preset step sizes. To ensure the proper resolution of data, a hemispherical sweep with steps of 5 degrees was used to establish the constant diffuse reflectance value. A high-resolution sweep in 0.5-degree increments was then run around the approximate peak of reflectance to determine the peak value, peak location, and width of the specular reflectance. The computer would record the vertical and horizontal angle positions, the measured BR, and the calculated BRDF for each position into a table of values for the sample being measured.

2.3 Data Processing

The bidirectional reflectance maps made with the gonioreflectometer were processed to determine the total reflectance and the width and height of the specular component needed to empirically describe the material reflectance characteristics. The 5-degree hemispherical sweep was first averaged to determine the constant diffuse component. This averaged diffuse reflectance value was important because this constant was integrated over the hemisphere when

calculating the total reflectance and it was also subtracted from the specular peak during the process of fitting a Gaussian curve to the data. During initial analysis of materials with known reflectance greater than 90%, we found that, if the baseline was not carefully analyzed, the total reflectance could easily be calculated as being larger than 100%. We developed procedures to ensure that all of the processed points were valid.

There were many measured points in the hemispherical sweep which were known to be sensitive to small errors and, as such, were cut from the data to ensure that these values did not skew the baseline reflectance value. A computer program was written to process the hemispherical sweep data and produce a baseline reflectance value. The program first averaged all points in the data set and provided an initial baseline reflectance value. Next, three types of points were deleted from the data. The first set was all the points between 85 and 90 degrees vertical angle. Since the BRDF was calculated by dividing the BR by the cosine of the vertical angle (as this angle approaches 90 degrees where the cosine becomes zero), the result can be sensitive to variations in the equipment. The second type of points to be discarded were all the points believed to be in the specular peak. The third type of points removed from the data were due to the design of the gonioreflectometer: there were positions at which the vertical arm that holds the photoreceptor partially blocked the light from the incident light source. At these locations, the apparent intensities dropped artificially lower than the baseline reflectance value if these points were included in the calculation. For material samples which consisted only of diffuse reflectance such as flat paint samples, a forward scattering peak was observed at angles significantly greater than where the specular peak should occur. This anomaly is discussed in Section 2.4. Once all sets of erroneous points were discarded, all the remaining points were averaged for the constant diffuse reflectance value.

The graph in Figure 2.4 shows features of the raw data that had to be omitted. "**A**" points to the 90-degree vertical angle data which was always zero, "**B**" points to the artificial rise in BRDF at a vertical angle of 85 degrees, "**C**" points to the forward-scattering peak in a flat paint sample, and "**D**" points to the regions obscured by the gonioreflectometer geometry.

Once the diffuse reflectance value was determined, the fine angular sweep was used to determine the width and height of the specular component. An anomaly with the gonioreflectometer created hysteresis in the data on the horizontal sweep. The peak of the data, which should have been around $\theta_r = 45$ degrees, would change between 1 to 3 degrees from the positive to negative vertical sweep to the negative to positive vertical sweep. If the peak in the forward sweep was at 45 degrees, the peak in the reverse sweep could be at 48 degrees, while the peak in the very next forward sweep would be back at 45 degrees. This effect would artificially give a wider distribution of data points. A program was written that would shift the reverse sweep points to the peak location of the forward sweep. The program required that the number of degrees that the reverse peak was shifted to be known. We determined this by visually looking at the raw data to find out how far off the peak in theta was from the zero degrees phi position for several degrees in phi in each direction. There was some error in this operation as it was assumed that the shift was constant throughout the data. A new file with the corrected data was created and used in further data processing.

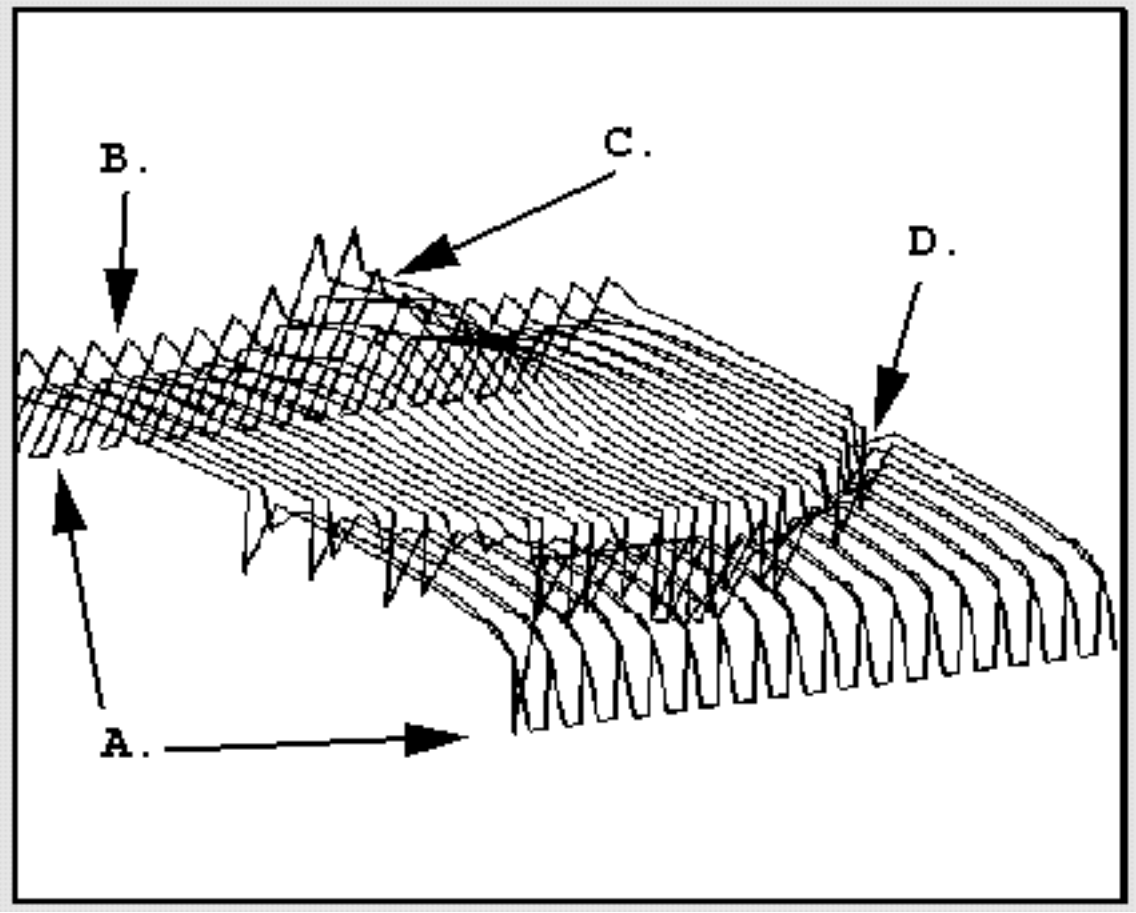

Figure 2.4: Graph of raw data for a flat sample.

The 3D data set (shown in Figure 2.4 for a diffuse material) was reduced to a 2D plot by assuming that there was symmetry direction about the Gaussian peak. The intensity for each point was plotted against the angle between the peak angle and the vector yielding a 2D plot of the data. Figure 2.5 shows a 2-D plot of a material with a specular component. We performed a fit to the 2-D Gaussian, after subtracting the constant diffuse value.

To ensure that the gonioreflectometer geometric calculations of the photodetector and light angles are correct, the sample material must be positioned at the correct height in the gonioreflectometer with no bends or wrinkles. These factors could not be controlled as precisely as was needed. To correct for this, we allowed an artificial shift in the location of the peak intensity value, and conducted a search for the best Gaussian fit to the data over a small range of shifted peak locations. This "best fit" Gaussian peak amplitude and width, along with the constant diffuse component, was used to generate the actual parameters needed for Radiance. These parameters are the total reflectance, the amount of this total reflectance which is specular and the width of the specular distribution.

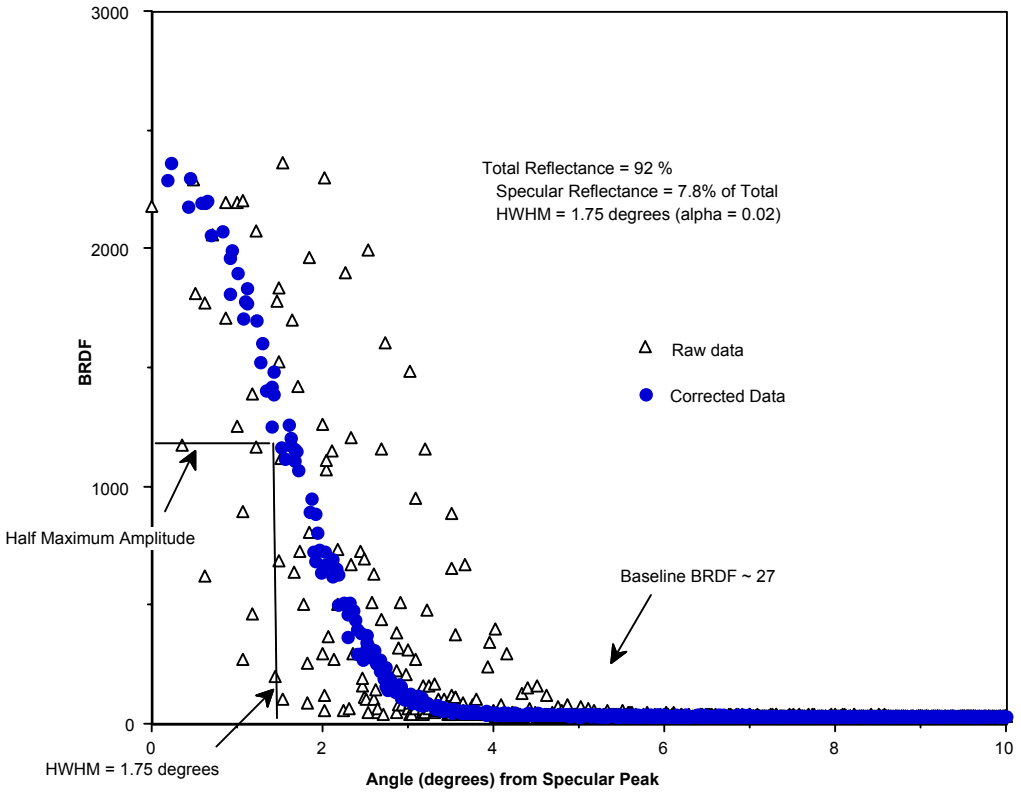

Figure 2.5: Corrected and raw data for exterior paint #Z202.

Figure 2.5 shows a plot of the gonioreflectometer data for the measurement of the specular components for Z202 gloss exterior white paint. All data are converted into the 2D projection where the angle plotted is the angle from the expected specular peak determined by the angle of incidence. The raw data show the broad spread in values about the peak. This spread is due to hysteresis between the forward and backward sweeps as discussed above and to errors in aligning the paint sample correctly in the gonioreflectometer. The corrected data lie on a well-defined Gaussian distribution allowing the height and width of the specular component to be determined. The HWHM is calculated by finding the angle in the Gaussian fit where the BRDF value is half the value at the Gaussian peak. Note that all data processing has assumed that the material reflectance is isotropic.

Some materials, such as the International Space Station (ISS) debris shielding with a brushed surface, have reflections which depend on orientation of the sample (anisotropic). These surface properties produce elliptical instead of spherical reflectance. We found that this 2D plot provided an easy method of determining whether the material reflectance had an anisotropic (elliptical) specular reflectance component. If only a small scatter in the Gaussian width remained after corrections, we assumed that the specular reflectance could be modeled as being isotropic.

2.4 Results and Conclusions

The results of these measurements have been catalogued in a computer database GRAF uses when computing luminance images. The database includes measurements of the following:

- ISS interior paints on aluminum and plastic bases
- ISS exterior materials, including debris shielding and EVA handrails
- Space Shuttle exterior paints
- Space Shuttle external reentry thermal protection, including tiles and thermal blankets
- Payload materials, including the Hubble Space Telescope (HST) photovoltaic power cells

The following paragraphs summarize general conclusions made from the measurements of these materials.

We found that the measured specular widths of the paint sample could be grouped according to gloss or semigloss. A statistical analysis of the paint samples found a mean HWHM of 1.64 $\pm$ 0.20 degrees for all gloss samples, and 5.464 $\pm$ 2.06 degrees for semigloss samples. Although many of the flat samples did have some increase in intensity near the specular peak, the width of this distribution was extremely large. Thus all flat samples are treated as being entirely diffuse. Student t-tests showed that, for the interior paints, there was no statistical difference between the samples painted on the aluminum surface vs. the samples painted on the plastic surface. The t-tests also showed that there was no difference between the interior and the exterior gloss paint samples. From the results of the gloss samples, it is clear that, as long as the paint is thick enough to completely cover the surface to prevent reflections from the material surface on which the paint is applied, then the under surface can be ignored in the calculation of reflectance.

It is important to note here that all of the interior paints used on ISS are specified by SSP-50008 as semigloss paints but, upon visual inspection, we decided that the samples provided had been painted with the gloss version of these paints. A visual comparison of the 27925 interior sample to the 17925 and 27925 exterior samples show that the 27925 interior sample more closely matches the 17925 exterior sample than it does the 27925 exterior sample. Testing of the samples verified that the half angle for all of these samples was more indicative of a gloss paint. Investigation into this divergence confirmed that the wrong paint type was being used in the NASA Space Station Mockup and Training Facility (SSMTF) for whom these samples were fabricated. Because of this, the sample numbers were changed to indicate them as being gloss samples, and were compared against the exterior gloss samples.

Another phenomenon, shown in Figure 2.6, is that almost all of the diffuse samples, flat paints, and materials such as the payload bay liner had a forward-scattering peak in the +60 to +85 degrees vertical range as shown in the uncorrected data for a typical flat sample in Figure 2.4. The cause of the peak is not apparent. It could be an equipment anomaly as the values being measured are low enough that light leakage and secondary reflections off of the equipment surfaces are larger than expected.

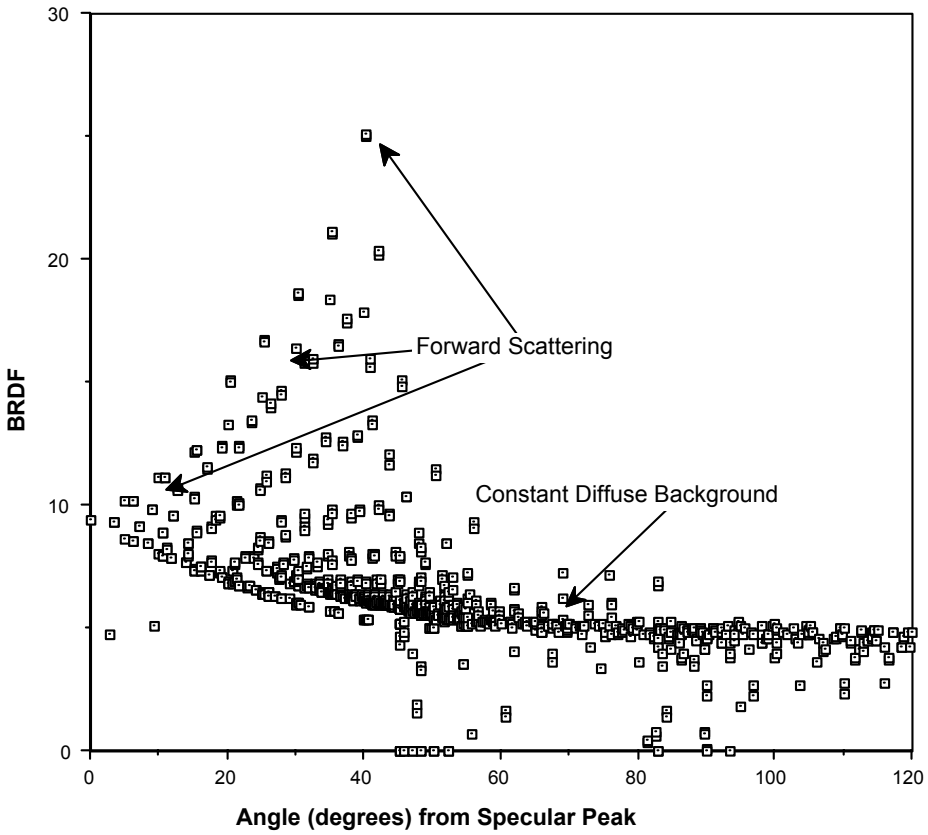

Figure 2.6: A 2-D plot of hemispherical data showing the forward scattering of light in diffuse samples. The plotted angle is the angular distance from the specular peak.

The gloss paints were found to have very similar specular widths and, because the total reflectance for paints is usually known, the need for expensive gonioreflectometer tests for paints may no longer be necessary. With the HWHM for gloss paints established along with the known total reflectance (which is part of the paint number), an easy measurement of the peak and baseline values might be taken with a spotmeter to obtain the information needed to calculate the percent of the total reflectance that was specular. Unfortunately, we found it very difficult to set up the precise geometry necessary to accurately measure the peak amplitude. However, with care, a "quick" estimate could be obtained from a paint sample in the field with simple and portable instrumentation.

3.0 Lamp Intensity Distribution Data

3.1 Theory

There are various ways of modeling the light distribution from a lamp assembly in a lighting calculation such as Radiance. If the lamp contains a filament and a reflector, it is possible to model each of these components and allow the uniform light distribution from the filament to be reflected from the reflector surface, thus producing a correct light distribution at a distance from the lamp assembly. This representation of a light is computationally intensive, resulting in slow generation of a complex image. The Radiance program allows a lamp to be modeled as a flat surface representing the front face of the lamp and associates an equation describing the distribution of the light on this flat surface. This description allows an accurate and rapid calculation. Data needed to use these equations for a lamp are the surface area of the lamp, the radiance of the lamp (watts/sr-m^2), and a table of the relative luminance intensity as a function of angle from the surface normal.

3.2 Data Collection

Many of the lamps used in the NASA space program have specification sheets. These sheets include graphs showing the illumination from the lamp as a function of angle for a given distance. When these data are available, they are used to determine the parameters needed for Radiance. When these data were not available, or it was suspected that the lamp and fixture did not meet the data in a specification sheet, the distribution of light intensity was measured in the LETF. A standard method of illumination measurement in the industry is to use a light goniometer [6]. A light goniometer places a light source at the center of a sphere and uses photocells to take illumination measurements along the inside of the sphere. While this method provides accurate measurements in an entire sphere around the source, it is an expensive piece of hardware. Various other methods can be used to gather similar data when a light goniometer is not available. Two methods are often employed in the LETF to supply Radiance with the information needed to simulate a source.

The first method measures the radial illumination distribution on a flat surface (Figure 3.1). The source is mounted perpendicular to a vertical wall board which has circular markings to define points at which an illumination measurement is to be made. A Photo-Research model 301 photometer/radiometer with a 160-degree acceptance angle cosine corrector attachment is held flat against the wall board, facing the light. The illumination in foot-candles for each point on the grid is recorded to measure the incident light from all directions.

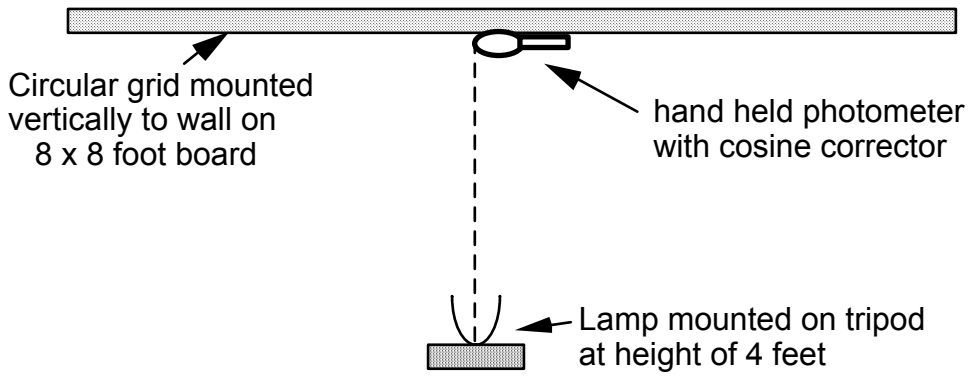

Figure 3.1: Top view of the experimental setup for a measurement of the illumination distribution.

The second method measures the illumination distribution as a function of angle at a fixed distance (Figure 3.2). The lamp is mounted perpendicular to a vertical wall on a tripod with a rotating plate which allows the lamp to be rotated up to 360 degrees. The illumination in foot-candles as a function of angle from the light normal is measured with the Photo-Research 301 cosine-corrected photometer/radiometer placed at the wall. This measures the lamp distribution in the horizontal plane only. To measure a vertical plane, it is necessary to turn the lamp on its side and repeat the process. We used this technique to measure the four lamps shown in Figure 3.3. This direct method eliminates calculation errors and allows large angular distributions to be measured.

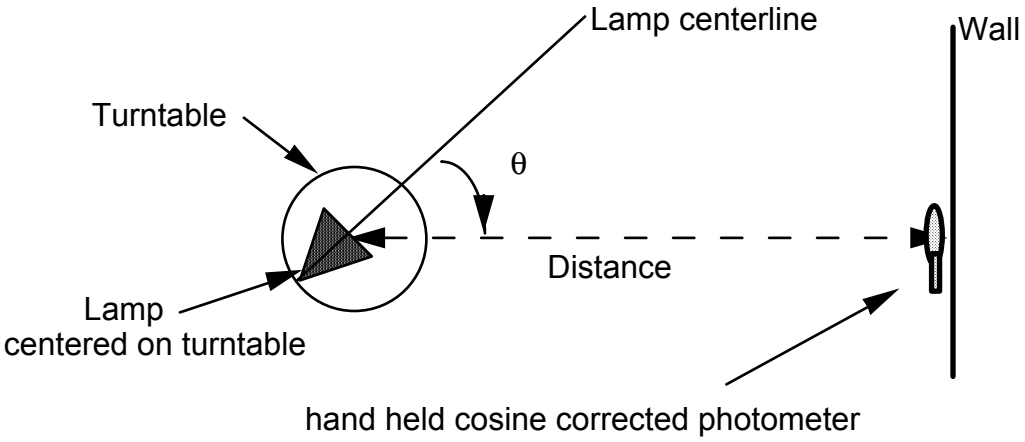

Figure 3.2: Experimental setup for measurement of illumination distribution as a function of angle (top view).

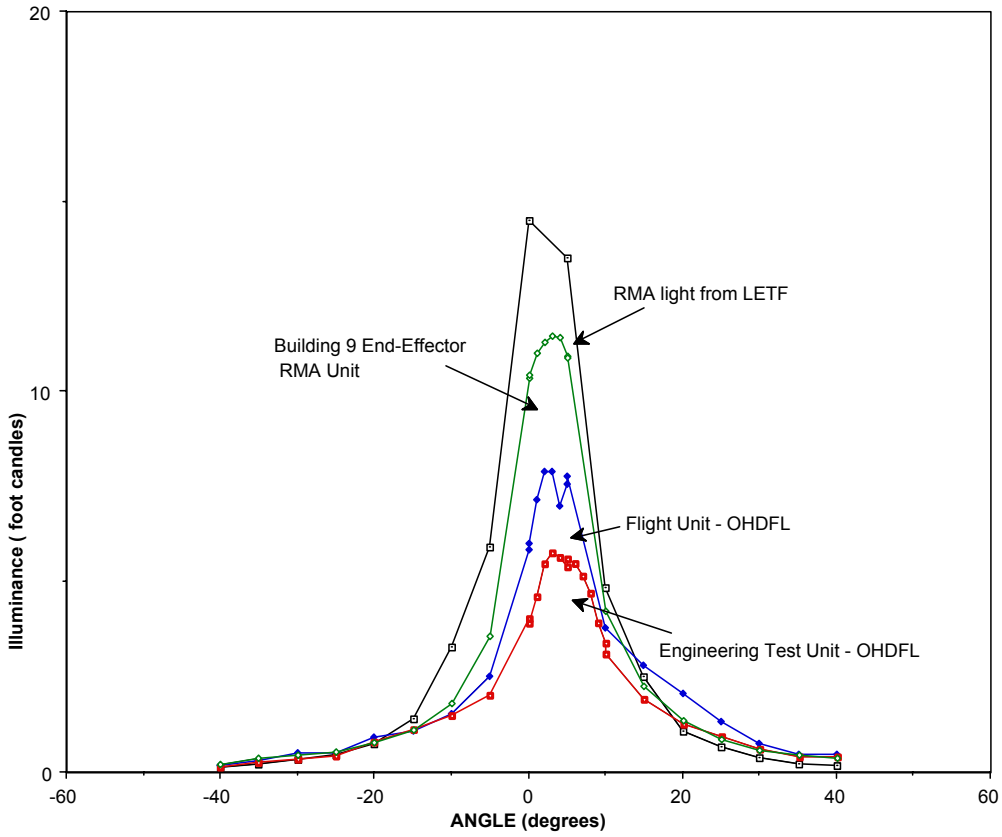

Figure 3.3: Illumination distribution measurements for the 4 test lights used for the mockup of STS-74 docking target tests.

3.3 Data Processing

The only processing needed for the measurement of light sources is to convert the data from the flat wall data collection method into illumination as a function of angle at a constant distance from the light. The flat wall method was generally used when this type of information was requested as it was for measurement of the extravehicular mobility unit (EMU) helmet light assembly where the distribution of light on a work surface needed to be determined. In order for Radiance to simulate the EMU helmet light, these data must then be converted into illumination as a function of angle at a constant distance from the light. Using the inverse square law, the illumination at one distance can be converted to illumination at another distance:

inverse square law $$F_c = \frac{CP}{D^2}$$

where F_c = foot-candles
CP = candlepower
D = distance

3.4 Results and Conclusions

Results for the measurement of standard NASA light sources for Space Shuttle and Space Station are detailed in Appendix B. As much information as could be obtained for each light is included. Some lights are specified by peak foot candle illumination at a specified distance. To get a peak illumination at another distance, the inverse square law can be used.

Due to limited wall space within the LETF, large angle lamp distribution measurements could not be completed. Therefore, the flat wall method is only used when NASA customers prefer data measurements of this type for their analysis. When describing the angular distribution of a light, it is necessary to have the angular illumination values at the same distances. Table 3.1 shows the conversion of the EMU helmet light flat wall measurements to radial measurements.

Table 3.1: Converting Radial Illumination Distribution Measurements to Angular Illumination Distribution

Measured Illumination (fc)	Wall Distance From Light Centerline (in.)	Angle From Light Centerline (degrees)	Radial Distance From Light to Wall (in.)	Ratio of Square of (Radial Distance/60)	Corrected Illumination at 60 Inches (fc)
1.7	0	0	60	1.00	1.70
1.45	6	5.71	60.3	1.01	1.46
1.29	12	11.31	61.19	1.04	1.34
1.06	18	16.70	62.6	1.09	1.16
0.85	24	21.8	64.6	1.16	0.99
0.52	36	30.97	69.98	1.36	0.71
0.51	48	38.7	76.9	1.64	0.67

Notes: Proposed new EMU floodlight with a 93 Parabolic Reflector TSC.
Center line distance from lamp to wall = 60 inches.

A comparison of the illumination as a function of angle from the light centerline for the two new EMU lights, the spotlight and the floodlight, shows two very different distributions which use the same lamp with different reflectors. The spotlight uses a reflector to focus the light along the lamp centerline, with most of the light within a cone of 20 degrees. This light peak illumination was measured to be 5.4 foot-candles at a distance of 10 feet. The floodlight uses a different reflector that spreads the light as uniformly as possible over a large area. The peak illumination

is much less, but the illumination has dropped to only half its peak over a cone of 80 degrees. Two of these helmet lights provide greater than 10 foot-candles over a work surface at 2 feet from the lights.

Very often a measured light distribution does not match the information on the specification sheets because not all lamps of a given type will have the same distribution or peak intensity due to variations in manufacturing. Also lamps degrade in intensity due to irregular cleaning, variations in power supplies, and age. Two remote manipulator assembly (RMA) lights and two overhead docking floodlights (OHDFLs) were measured in the LETF. Figure 3.3 shows the results of these measurements with the differences in illumination clearly shown. The range of uncertainty in lamp luminance will limit the level of accuracy obtainable with the lighting calculations. However, all artificial light sources used on the Space Shuttle or Space Station have specified minimum accepted illumination levels. When operational lighting systems reach the minimum they should be replaced with new units. The appendix is a summary of lamps used in the space program.

4.0 Validation of Computer Luminance Calculation

When accurate lamp and material properties, along with accurate geometric objects, are incorporated into the Radiance lighting calculation, the computer calculation of the luminance from each surface in the scene should agree with measured luminance values within the limits of accuracy of the model and the measurements. Comparisons between calculated and measured values must be made with some understanding of the limitations in both: light sources may not have uniformly regular distributions; lamp intensities degrade over time; material surfaces may be non-uniform, and slight errors in orientation of lamps or surfaces can result in significant differences in measured luminance values.

Three earth-based tests have been used to check the luminance calculations against measured values. Two of these experiments were concerned with illumination conditions which can occur during the Shuttle-*Mir* docking. GRAF and LETF personnel were able to attend ground-based tests and make non-intrusive measurements during these tests which simulated Shuttle exterior lighting conditions in space. The third test measured interior lighting levels in the HAB module of the SSMTF located in Building 9A at JSC.

These three tests provided validation of the modeling under different lighting conditions. The first test used the solar simulator to model the effects of direct sunlight on a docking target. The second test used Shuttle RMA lights on the docking module to simulate exterior Shuttle lights. The third test used interior station fluorescent lighting in a small contained area where multiple reflections from surfaces are important.

4.1 Direct Sunlight Illumination of a Docking Target

This experiment was set up in the high-bay area of Building 44 (Figure 4.1). The walls in this area are painted black and black curtains block off the open areas. No windows are present in

this area, allowing illumination experiments to be conducted during the day. The experiment was to determine the sun angles at which washout of the docking target and standoff cross occurred. This washout occurs when the reflected light from the target and surrounding structures becomes large enough to produce a vailing luminance into the television camera lens.

The solar simulator was positioned on a cart at a radial distance of 10 feet from the docking target. The docking target assembly, consisting of the black standoff cross, white back plate with black alignment markings, was mounted in the mockup of the *Mir* docking port representing the STS-71 configuration. A solid-state color tv camera (CTVC) was positioned in line with the docking target at a distance of 16 feet. The solar simulator was directed at the target at angles between 60 and 85 degrees. Test subjects viewed the CTVC image on Shuttle CRTs to evaluate whether the black cross and alignment marks were discernible or "washed out." A Photo-Research Spotmeter (PR 1500) was mounted on a tripod next to the CTVC. At each sun angle, measurements of the luminance (foot-lamberts) from the white back plate region and from a section of the aluminum hatch structure behind the white target were made.

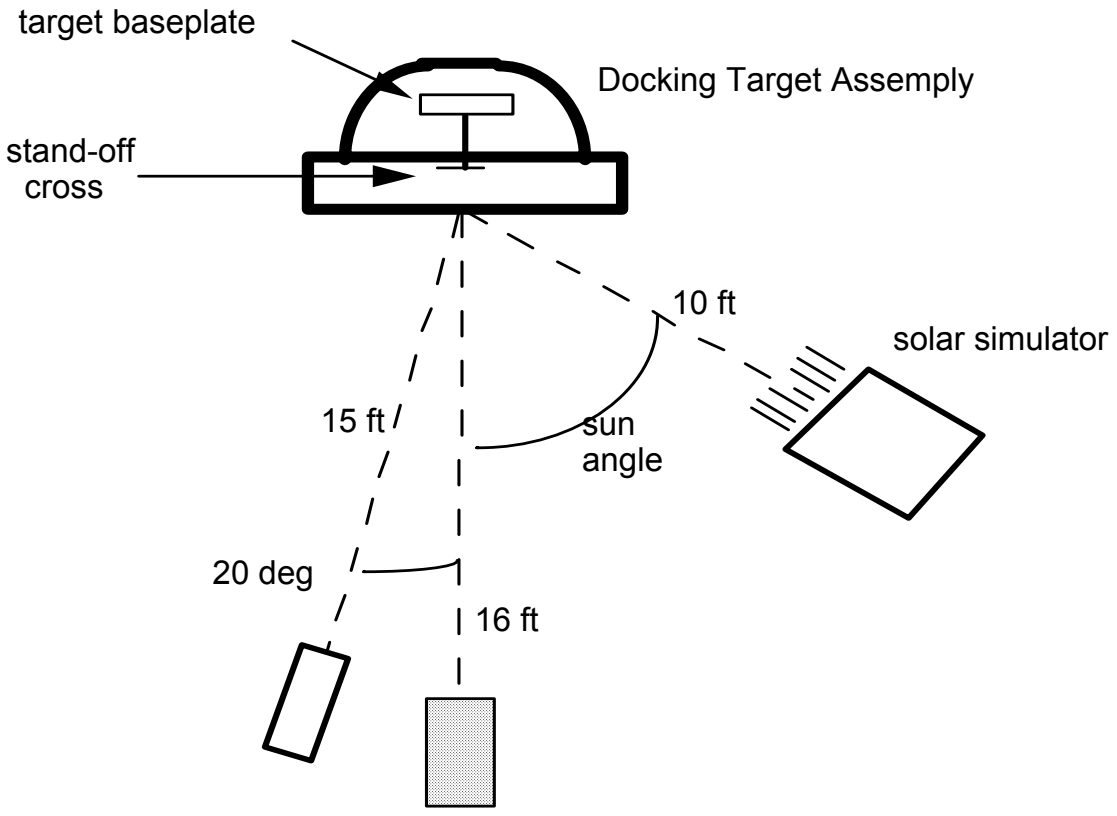

Figure 4.1: Building 44 test setup.

To compare these measurements with the Radiance luminance calculation, we created a graphical model of the test geometry. The solar simulator was modeled as a uniform light with a 3-degree beam spread with the light dropping to zero at angles off axis greater than 5 degrees. A lighting image, generated for each sun angle, contains the luminance value for each pixel in the

image. The average luminance over the 1-degree field of view of the photometer, along with a maximum and minimum luminance, were determined from the computer image. Figure 4.2 shows the comparison of the calculated luminance with the measured luminance. The luminance values are plotted on a log scale to plot the large range of values that were measured. Figure 4.3 shows the computer image compared with a video camera image. The comparison between measured and calculated luminance shown in Figure 4.2 shows significant agreement. A major source of error in the calculation was the modeling of the solar simulator. We assumed the distribution of the solar simulator was constant over the center region, but when the solar simulator was directed onto a flat diffuse surface at a distance of 17 feet and the illumination measured at various positions within the visible region, the values ranged between 3,000 and 5,700 foot-candles. This irregular illumination reduces the accuracy between the calculations and the measurements.

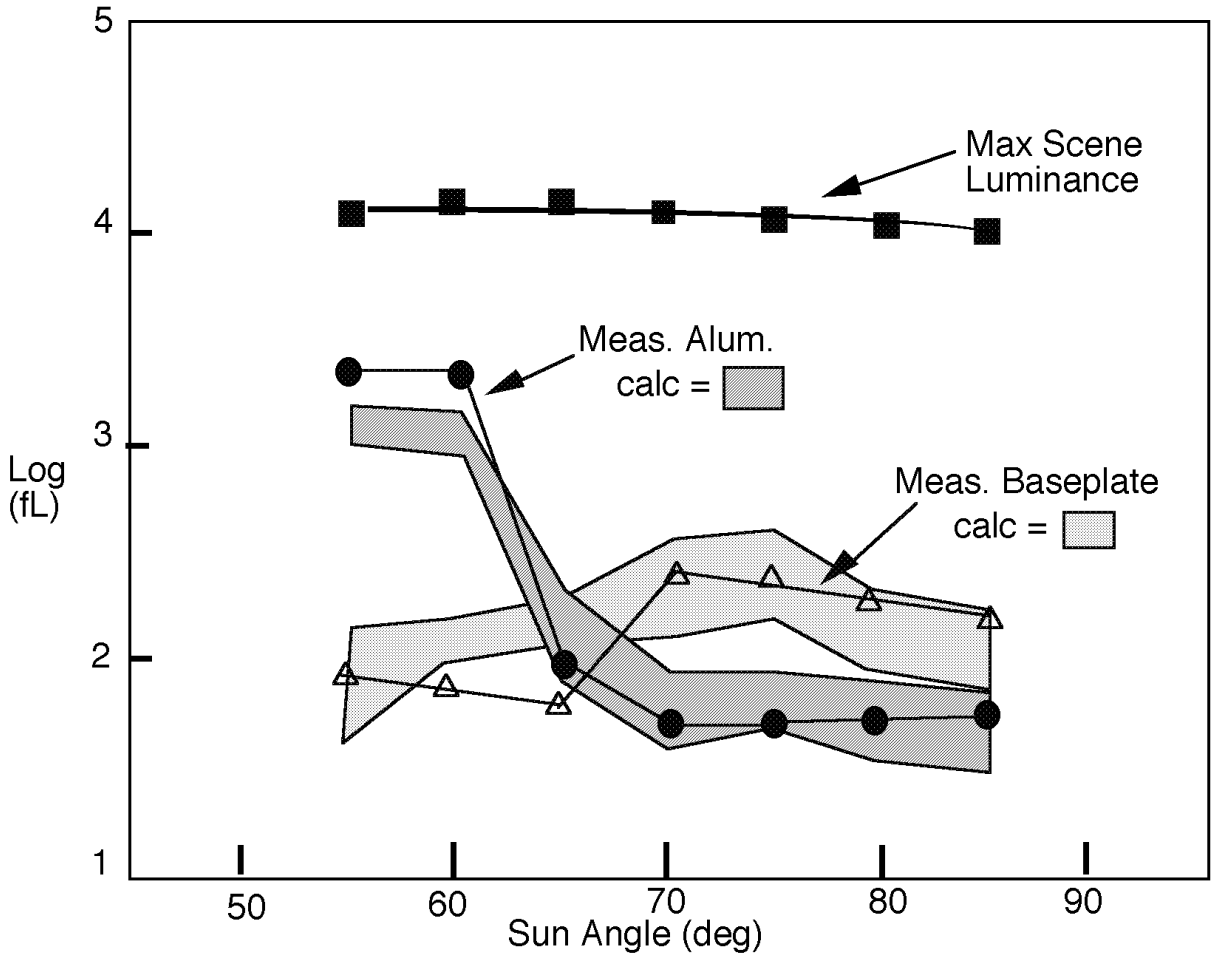

Figure 4.2: Luminance measurements and calculations plotted for comparison. The "baseplate" is the diffuse white plate behind the black standoff cross. The "Alum" is the specular aluminum metal surface behind the white baseplate.

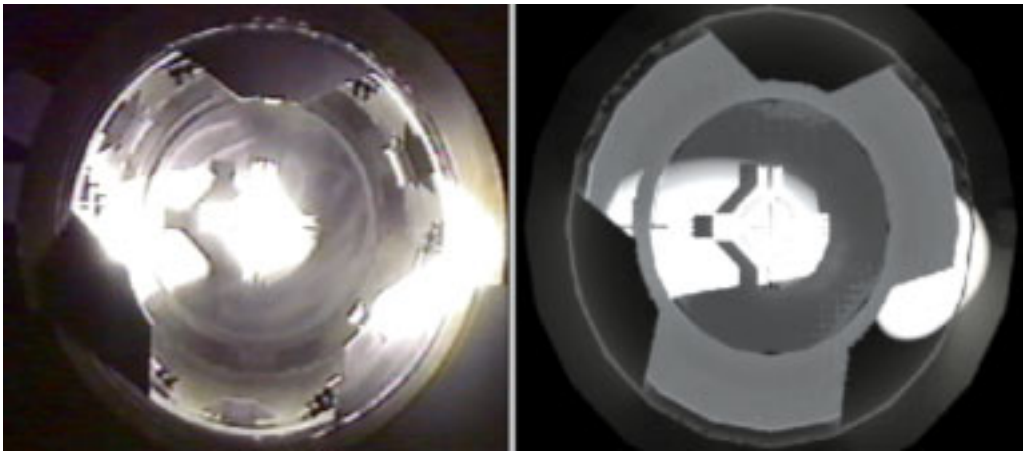

Figure 4.3: Computer image (right) compared with a video camera image (left).

4.2 Exterior Shuttle Lighting

This test was conducted at JSC in Building 9A. This facility provided a much longer viewing distance for the CTVC than could be provided at Building 44. A cart was built to represent the Orbiter side of the docking assembly which has 4 RMA lights (2 truss and 2 vestibule), a CTVC, and a monochromatic lens assembly (MLA) camera. The *Mir* docking assembly was the same as the one used in the direct-sun lighting test, except that the target back plate was configured to represent the STS-74 target. The "Orbiter" cart was moved to distances between 60 and 10 feet from the *Mir* docking interface. The TV cameras monitored the target image to determine the maximum distance at which the target black indices and the standoff cross alignment were discernible.

These tests were run using both the CTVC and MLA cameras. Runs were made using various lighting combinations. Additional washout tests, similar to the Test 1 experiments, were performed using the solar simulator. The PR 1500 was set up at a distance of 20 feet from the target and at an angle of 30 degrees from centerline. Luminance measurements from the white back plate were made for each test position. Figure 4.4 shows the setup for this test.

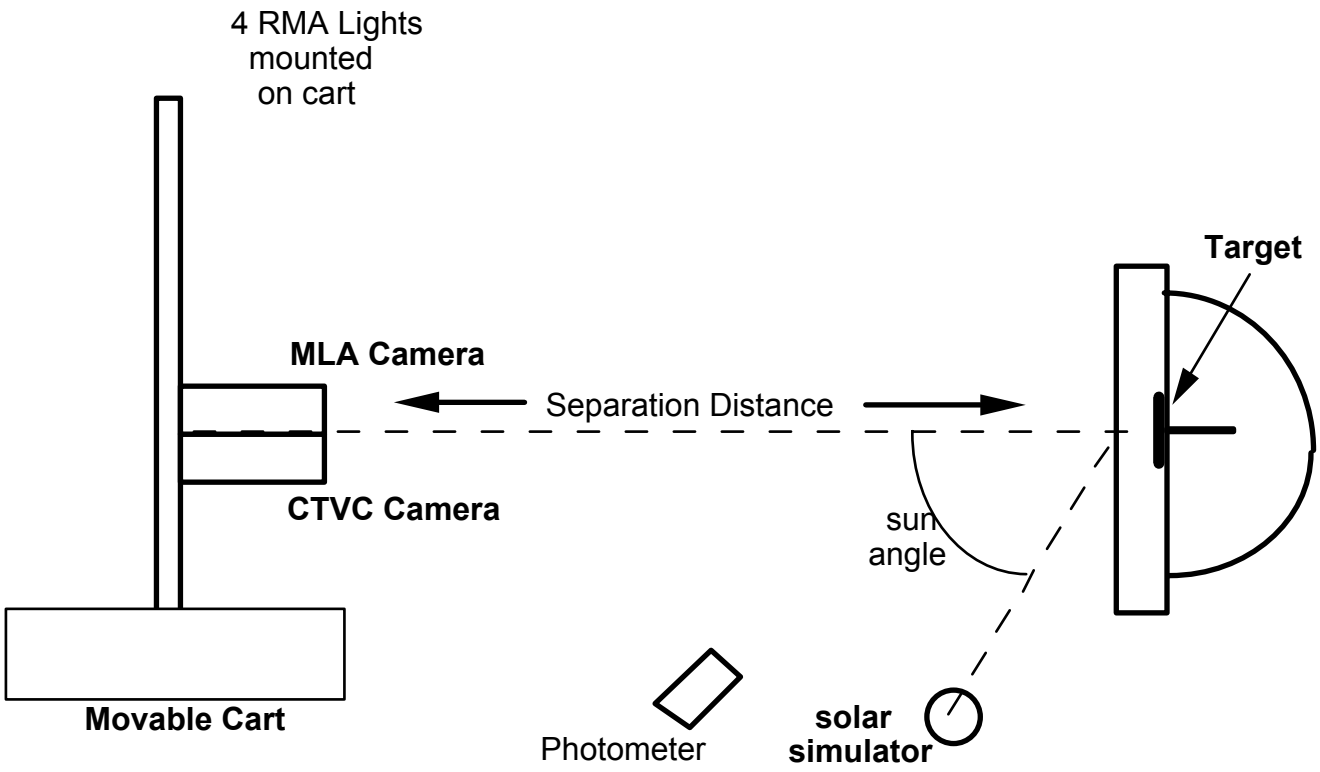

Figure 4.4: Experimental setup for exterior Space Shuttle lighting test.

This test was conducted over a two-night period, allowing collection of a large amount of data. Since the direct-sun lighting test used the solar simulator for validation, the main interest of this test was to validate the lighting calculation when using artificial lights. Before the test was conducted, luminance calculations were made to predict luminance values which would be measured. For these calculations, we used the standard RMA light, with a design specification of 12 foot-candles at 15 feet, for all 4 lights. Figure 4.5 shows the comparison of the measurements with this precalculated data. The agreement was within 2 foot-lamberts of the measured data. After the test was conducted, the 4 lights used in the test were taken to the LETF for measurement. These measurements revealed that the 4 lights had very different peak illuminations. Using these new lamp measurements to model each light, the new calculation of luminance values has the same slope as the measured values, but lower by a constant offset. This offset could be due to either an incorrect reflectance value for the white baseplate or the ambient background light in building 9A. This building has white walls, ceiling, and full-size Shuttle and payload-bay mockups which result in significant light scattering. Background illuminance levels around 0.9 foot-candles have been measured at the Space Shuttle during a similar lighting test. As this additional scattering would not be present in space, it was not incorporated into the computer model.

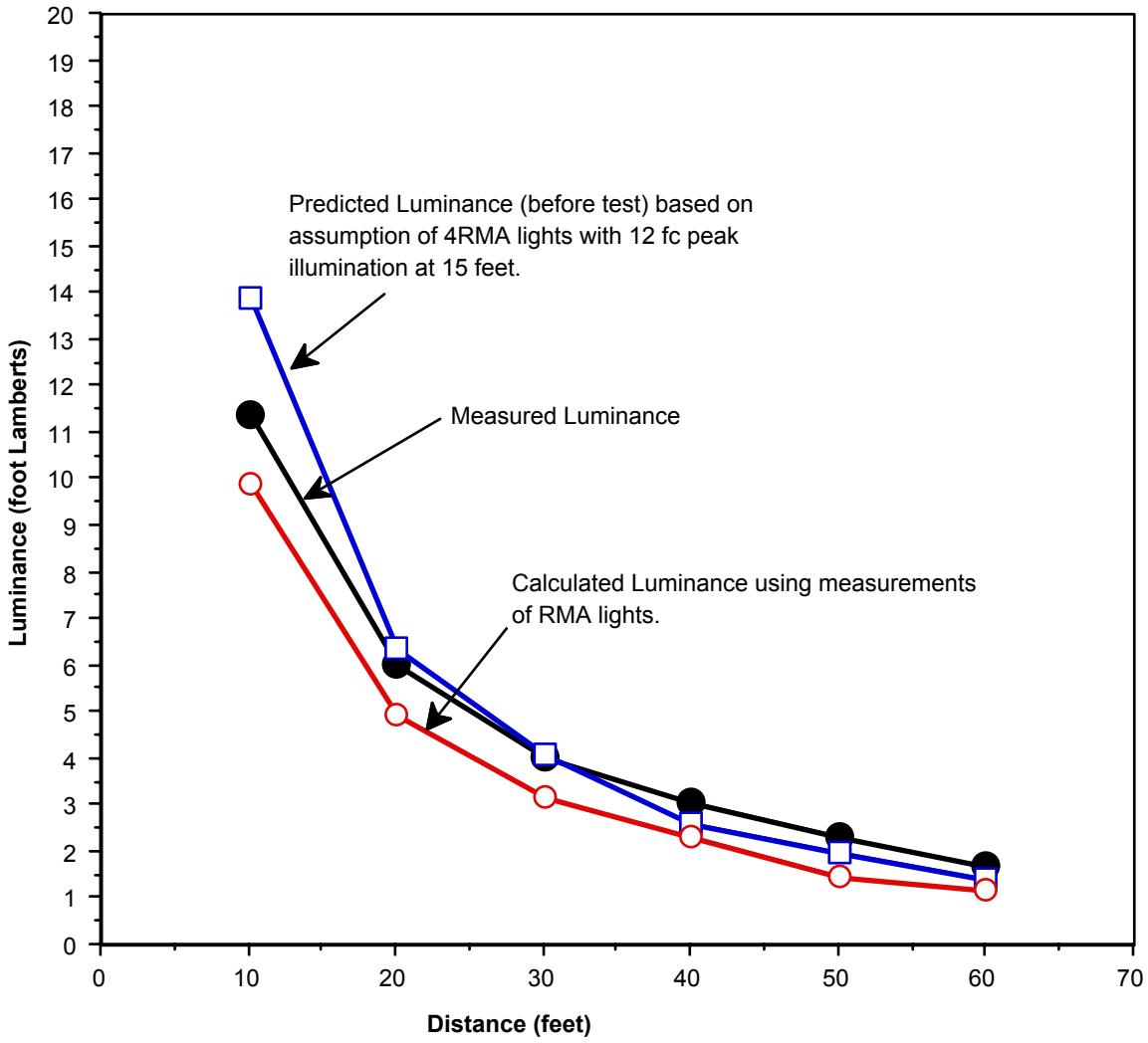

Figure 4.5: Calculated and measured luminance from the white diffuse baseplate behind the black standoff cross target.

4.3 Interior Space Station Lighting

The first two tests were simulations of exterior lighting. When a light ray is reflected from a surface in open space, the probability of striking other objects is reduced. Thus lighting calculations can be modeled accurately even when limiting the number of reflections that are allowed. This limitation in the number of reflectances makes exterior Shuttle/Station computer calculations with very complex geometry possible in a reasonable length of time. However, when modeling interiors of rooms, a light ray will be reflected from surfaces many times before its contribution to the lighting becomes negligible. To check that the Radiance program can be used to calculate lighting levels for interior regions, we used a mockup of the HAB module located in the SSMTF to gather interior lighting data.

The interior of this module resembles a long rectangular room, formed from the faces of 24 racks along the walls, ceiling, and floor, 6 on each side. The basic room size is 84 x 84 x 240 inches. Twelve fluorescent lights are mounted in the recessed areas between the walls and ceiling. The mockup has many details such as consoles, drawers, and knobs which were not modeled in the computer image. These details were not assumed to be a major influence on the overall illumination levels. Illumination and lumination data were collected at various positions in the room using a PR 301 foot-candle meter.

Figure 4.6 shows an RCA video camera image and a computer-generated image taken from similar viewpoints. Multiple images of the fluorescent lights can be seen on the hatch door at the end of the room in both views. The relative brightness ratios also appear similar. Computer images were generated using various numbers of reflections. The visual images changed greatly between 1 and 5 reflections. When only one reflectance is allowed, only direct illumination is seen, causing the illumination across the rack surfaces to vary. When 5 or more reflections are allowed, the illumination across the rack surface becomes nearly uniform.

Figure 4.6: Comparison of video camera image (right) and computer image (left).

A problem encountered with interior comparisons is related to how measurements are made, and how to model these measurements in Radiance. When a photometer with a narrow acceptance angle is used to measure luminance from a surface, the Radiance image is directly related to this luminance value. Table 4.1 shows the comparison between measurements and calculations of luminance in four directions using the PR 301 with a 10-degree acceptance angle attachment. Each measurement was taken with the photometer placed at the direct center of the HAB module pointing toward one of the four rack surfaces, ceiling, floor, right wall, and left wall.

Table 4.1: Luminance (Foot-Lamberts) Measurements and Calculations Using a 10-Degree Acceptance Angle Light Meter

	UP	DOWN	RIGHT	LEFT
Measured	5.3	10.2	7.3	7.2
Calculated	5.7	6.0	7.3	8.0
% Difference	7.5%	41.2%	0.0%	11.0%

The agreement between measured and calculated values is reasonable except for the measurements in the DOWN direction. For this measurement the detector was pointed down toward the floor. The floor in the HAB module is covered with a plastic sheet which was not included in the computer model. It is probable that the difference in reflectance from the plastic sheet used on the floor accounts for this larger luminance measurement.

Illumination measurements were also made with the PR 301 using the standard photoreceptor which has a 70-degree field of view. The method used for the previous luminance test was repeated for this illuminance test. Comparisons are made between the calculated and measured values showed agreement to about 14%. Table 4.2 shows this comparison.

Table 4.2: Measured and Calculated Illumination Values (Foot-Candles) Using a 70-Degree Acceptance Angle Light Meter

	UP	DOWN	RIGHT	LEFT
Measured	6.7	4.4	4.4	4.7
Calculated	6.6	4.1	5.0	5.2
% Difference	1.5%	6.8%	13.6%	10.6%

These measurements are difficult to make without the person making the measurements interfering with the light in the room. The person will almost always be blocking direct light from one of the 12 lamps. This process of measuring introduces errors. Also, when using a photometer with only a 10-degree acceptance angle, slight variations in aiming direction can make large differences in the readings. As long as the detector is not gathering direct lamp luminance or surface specular reflections, the errors in measurements should not be large.

Illumination measurements were made with a 160-degree cosine correction attachment. Most often, this attachment is used for illumination measurements because it gathers light over a large solid angle. Fish-eye radiance images were generated for comparison, but poor agreement was found. The 160-degree acceptance angle records several of the lamps at large cosine angles. If no correction to the calculations were made, then the calculated illumination was appreciably lower than measured. An attempt to apply a cosine correction to the calculations resulted in illumination higher than measured. Additional work is in progress to model the photometer illumination when the cosine correction attachment is used.

5.0 Conclusions

The reflected distribution of light from a large number of materials used in the Space Shuttle and Space Station programs were measured using a gonioreflectometer, and a process was developed to convert this data into Radiance parameters. A database compiled for these materials includes three parameters: the total reflectance from the surface, the percent of the total reflectance that is specular, and the angular width of the specular distribution.

A database of light values was compiled for most of the luminaires in the Space Shuttle and Space Station programs. Industry standard collection methods of light distribution data were used for lights when manufacturer specification sheets were not available. This database includes as much information about the light as could be gathered, including part number, location/use, size, power, peak illumination, and beam width.

Methods of predicting luminance levels have been shown to be reasonably accurate for a variety of lighting conditions, including direct-sun lighting and artificial lighting. The Radiance calculations have been shown to give good results for both exterior and interior lighting environments.

Future work should continue to update and expand this database to include more of the paints and structural materials as they become specified for the Space Shuttle, Space Station, and other future spacecraft programs.

Work has already begun to develop algorithms which will allow these luminance calculated images to be displayed as accurate simulations of the Shuttle cameras. Other flight cameras and camera lenses can display the same scene very differently. To predict when light levels are adequate for camera viewing, it is essential to model correctly how the calculated luminance image is displayed by the various cameras.

6.0 References

[1] Maida, J. C., Pandya, A. K. and Aldridge, A. M. (1992). A Comparison and Validation of Computer Lighting Simulation Models for Space Applications Using Empirically Collected Data. Research and Technology Annual Report 1992, II8-10.

[2] Ward, G. J., Rubinstein, F. M. and Clear, R. D. (1988). A Ray-Tracing Solution for Diffuse Interreflection. 1988. Computer Graphics, Vol. 22, 85-92.

[3] He, X., Torrance, K. E., Sillion, F. X., Greenberg, D. P. (1991). A comprehensive physical model for light reflection, Computer Graphics, 25(4), 175-186.

[4] Ward, G. H. (1992). Measuring and Modeling Anisotropic Reflection. Computer Graphics, 26, 265-272.

[5] Operation and Maintenance Manual for Automated Gonioreflectometer. (1989). Lighting Sciences, Inc.

[6] IES Lighting Handbook (1984). Kaufman, J. E., editor, Illuminating Engineering Society of North America, N.Y.

APPENDIX

Appendix A
Database of Lights

A wide variety of lights is used in the space program. These have been divided into 6 groups:

1. Exterior Space Shuttle lighting
2. Interior Space Shuttle lighting
3. Exterior International Space Station (ISS) lighting
4. Interior ISS lighting
5. Interior portable lighting, including flashlights
6. Exterior portable lighting. This group includes the extravehicular mobility unit (EMU) helmet lights and the high-intensity search light.

Each group has a summary table listing name of light, power requirements, lamp intensity or illumination, beam spread, size, and weight. The lamp manufacturer ID number is included when known.

The beam spread is defined as 2 numbers. The first number is the half angle at which the beam intensity is 50% of the peak intensity. The second number, inside of (), is the full extent of the beam distribution. Most lamps are assumed to have symmetrical distributions about the lamp centerline. Exceptions to this are fluorescent lamps and the ISS crew equipment translation assembly (CETA) external fixed lamp.

Table A-1: Exterior Space Shuttle Lighting

Name/Use	Power/ Volt	Peak Intensity	Beam Spread (degrees)	Type	Dimming	Size (inches)	Weight (lb)
Overhead Docking Floodlight MC434-0066 ILC 39820	130 watts 35 Vdc	4585 BCP max: 22 fc at 15 ft	+/-20(40)	Tungsten Halogen	no	6 x 4.5 x 5.0	8
Remote Manipulator Arm (RMA) Floodlight MC434-0063 ILC 38834	130 watts 28 Vdc	3490 BCP max: 16 fc at 15 ft	+/-20(40)	Tungsten Halogen	no	6 x 4.5 x 5.0	4
Forward Bulkhead Floodlight MC434-0065 ILC 36273	200 watts 28 Vdc	1195 BCP max: 7 fc at 12 ft	+/-60(120)	Metal Halide	yes with override	9 x 5.6 x 5	5
Payload Bay Floodlight MC434-0062 ILC 36267	200 watts 28 Vdc	1175 BCP max: 18 fc at 8 ft	+/-65(135)	Metal Halide	no	13.75 x 7.75 x 5.25	5

Notes: The Orbiter docking system (ODS) in the payload bay has 4 RMA lights. Beam candle power (BCP) is the averaged candle power over 50% of the lamp peak intensity.

Table A-2: Interior Space Shuttle Lighting

Name/Use	Power/ Volt	Peak Intensity	Beam Spread (degrees)	Type	Dimming	Size (inches)	Weight (lb)
Airlock and Middeck Panel Light MC434-0068-0109, -0119, -0120 ILC 36409	6.6 watts 28 Vdc	89 cp	+/-20(40))	5 inch T5/1 Fluores.	no	7x.85x2.51	1
Aft Work Station Floodlight MC434-68-0111 ILC 36412	19 watts 28 Vdc	435 cp	+/-80(160)	18 inch T8/1 Fluores.	yes with override	22x4.5x3.3	4.5
General Purpose Middeck Ceiling MC434-0068-0114 ILC 36415	16.5 watts 28 Vdc	210 cp	+/-60(180)	18 inch T8/1 Fluores.	no	22x4.5x3.3	4.0
Glare Shield Floodlight MC434-0068-0027-0127; -0028-0128 ILC 36417/ 36421	33 watts 28 Vdc	175 cp	+/-30(60)	5 inch T8/1 Fluores.	yes	19x4.26x1.38	3.0
Side Panel Overhead Light MC434-0068-0117,-0118, -0121,-0122 ILC #36424,-27,-33,-35	16.5 watts 28 Vdc	245 cp	+/-45(90)	9 inch T8/1 Fluores.	yes	13x2.62x2.55	3
Heads Up Display Light MC434-0068-0127,-0128, -0129,-0068-0029 ILC 36437, 36440, 36442	15 watts 28 Vdc	84 cp		5 inch T5/2 Fluores.	yes	8.2x3.16x0.875	1.0
Payload/Mission Specialist MS434-0068-0111	12 watts 28 Vdc	95 cp	+/-45(90)	18 inch T8/1 Fluores.	yes	22x4.5x3.3	4.5
High-Intensity Search Light Portable for Use With Orbiter Overhead Window ITL 33082	100 W	$1.2x10^5$ candelas 3 fc at 1000 ft	+/-1.25(2.5)	Tungsten Halogen	no	8" diameter	2

Table A-3: Exterior International Space Station Lighting

Name/Use	Power/ Volt	Peak Intensity	Beam Spread (degrees)	Type	Size (inches)	Weight (lb)
Video Camera Light; 4 to Be Used on ISS at One Time 14 Port Locations McDAC 9468	150 Watts AC	9.3 fc at 60 ft	±11 (22)	Metal Halide	10x16x16	32.5
CETA Light 2 for Sarj Crossing (P3, S3) 2 for Airlock/CETA SPUR (S0-LAB, S1) 2 for Node 1 ITL 44264	55 W Input; 40 Watts to lamp	8414 cp or max: 25 fc at 20 ft (Peak value not at lamp centerline)	+/-12(28.5) (approx.)	Metal Halide	11.4 dia. x 10	24
SSRMS Lights ILC 220582	80 Watts	370 cp	+/-26.2(53)	Tungsten Halogen	4x5x5.45	5.06

Table A-4: Interior International Space Station Lighting

Name/Use	Power/ Volt	Peak Intensity	Beam Spread (degrees)	Type	Size (inches)	Weight (lb)
ISS HAB-LAB General Purpose Light ILC 21903	20 W max 120 Vdc	190 cp	+/-25(70)	9 inch T8/1 Fluores	13x2.62x2.55	8.75

Table A-5: Interior Portable Lights (Space Station and Space Shuttle)

Name/Use	Power/ Volt	Peak Intensity	Beam Spread (degrees)	Type	Size (inches)	Weight (lb)
Personal Pen Light (battery)	2 AA cells	2200 candella	variable	Tungsten	7.4” length x .75” dia.	0.8
Equipment light (battery)	5 C cells	7627 candella	variable	Tungsten	15” length x ~1.85” dia.	~3
IVA Portable Utility Light (station power)	110 V AC Lamp: 12 Vdc	500 candella	+/-20(40)	Halogen	6" length x 3.25" x 3.25	2.9

Table A-6: Exterior Portable Lights

Name/Use	Power/Volt	Peak Intensity	Beam Spread (degrees)	Type	Size (inches)	Weight (lb)
EMU Helmet Floodlight	3.3 W, 3 Vdc 2 D-size Lithium Bromide batteries	20 fc at 2 feet 85 cp	+/-46(70)	Tungsten Halogen	0.875 dia.	
EMU Helmet Spotlight	2.9 W, 3 Vdc 2 D-size Lithium Bromide batteries	5.4 fc at 10 feet 510 bcp	+/-6(40)	Tungsten Halogen	0.875 dia.	
Hubble Space Telescope Portable External Light	28 Vdc	2280 candelas high set: 252 fc at 3 ft low set: 189 fc at 3 ft	+/-10(53)	Tungsten Halogen	4.5 dia.	6
High Intensity Search Light Portable for Use With Orbiter Overhead Window ITL 33082	100 W	1.2x105 candelas or 3 fc at 1000 ft	+/-0.6(3.5)	Tungsten Halogen	8" dia.	4

Note: The EMU helmet light assembly consists of 4 lamps, 2 on each side of the helmet. Usually, each side will have one floodlight and one spotlight. Only one light on each side will be turned on at the same time.